# Report on mechanical measurements in the main LHC dipole collared coils: October-November 2002

I.Vanenkov, LHC-MMS-MA

This report gives data concerning the mechanical measurements in coils inner and outer layers, assembled poles and collared coils.

## 1. Data of coil size measurements

- Firm 1 (ALSTOM) – up to date, 132 assembled poles are measured with the old press, the post-processing of raw data is done at CERN.
- Firm 2 (ANSALDO) – 50 assembled poles, starting from the pole P30 are measured with the new press (IMMG), 28 inner and 42 outer layers have been measured with the old press. The post-processing of raw data is done by ANSALDO personnel, using software provided by CERN.
- Firm 3 (NOELL) – 62 inner and 60 outer layers are measured with the old NOELL press; the post-processing of raw data is done by NOELL personnel, using software provided by CERN.

### 1.1 Coil layers and poles production rate

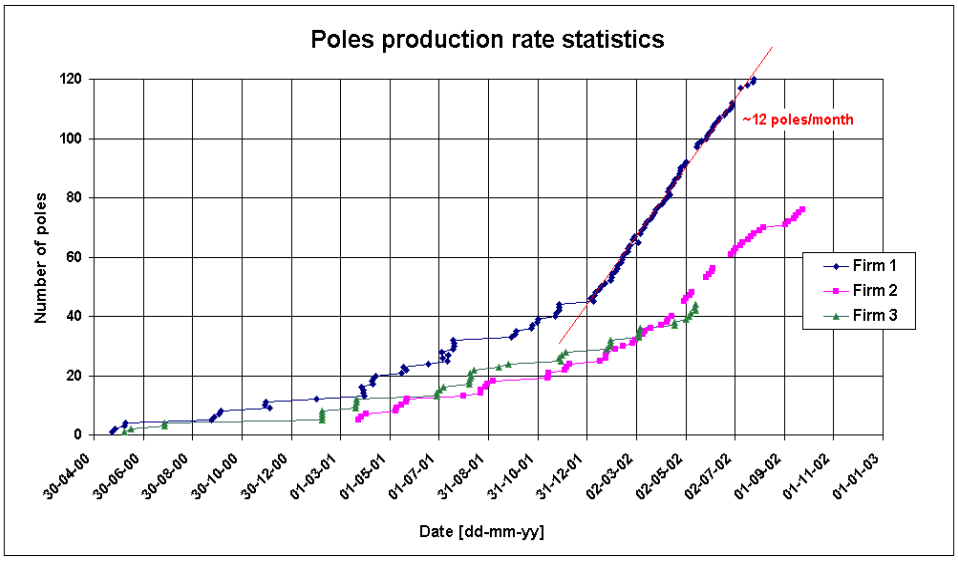


Fig. 1 Assembled poles production rate for three firms.

## 1.2 Trend graphs

### 1.2.1 Measurements on assembled poles

Firm 1. The data on the coil size shows a significant non-systematic variation (fig. 1). The coil size varies from –0.3 up to +0.2 of mm in a random way. For example: a drop in the inner layer coil size of the poles 58 – 60 can be observed as well as an increase on the pole 57. These 4 poles all belong to the same collared coil (CC-15), which is the last collared coil of *X-section 1* inner layer coil design. A similar case can be seen for the CC-17 (poles 65-68). The impact of these coil size asymmetries on the skew quadrupole (*a2)* is presented later in this report.

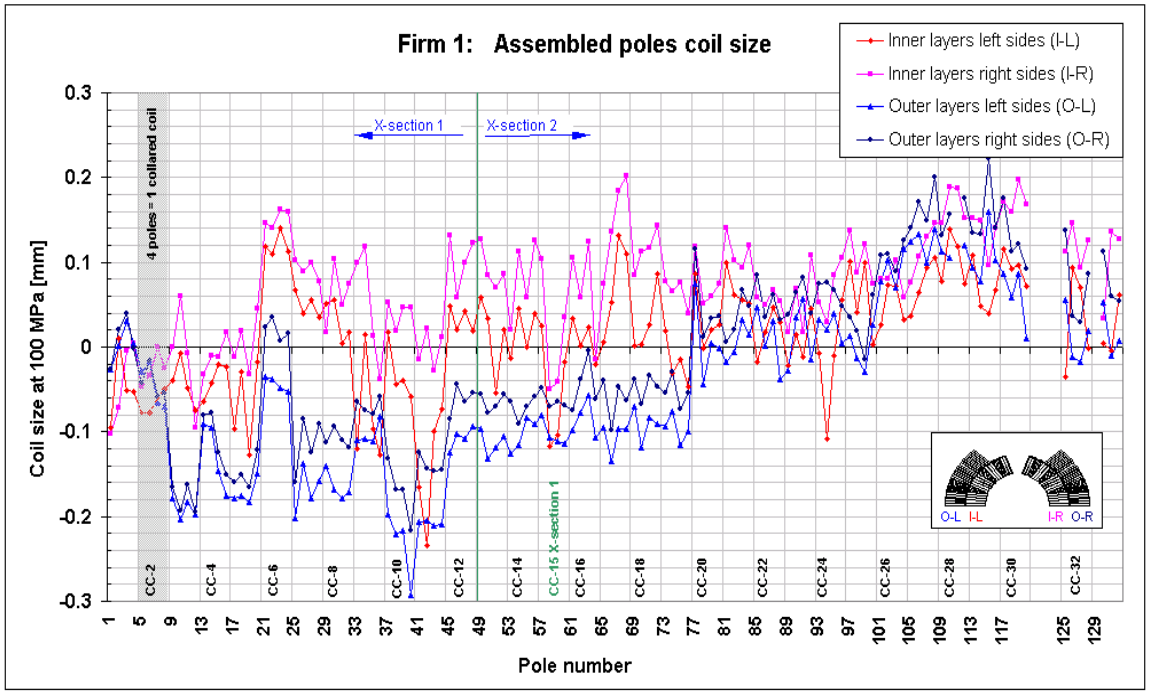


Fig.2 Firm 1. Average coil size in the straight part of the assembled poles (132 poles).

Firm 2. The variation in the coil size (see fig. 3) is smaller by almost a factor of two compared to the coils that are made by firm 1. However, a visible jump of almost 0.1 mm in the inner and approx. 0.08 of mm on the outer layers is observed, for the coils, starting from pole 45 on which is the first pole of the inner layer coil *X-section 2* design.

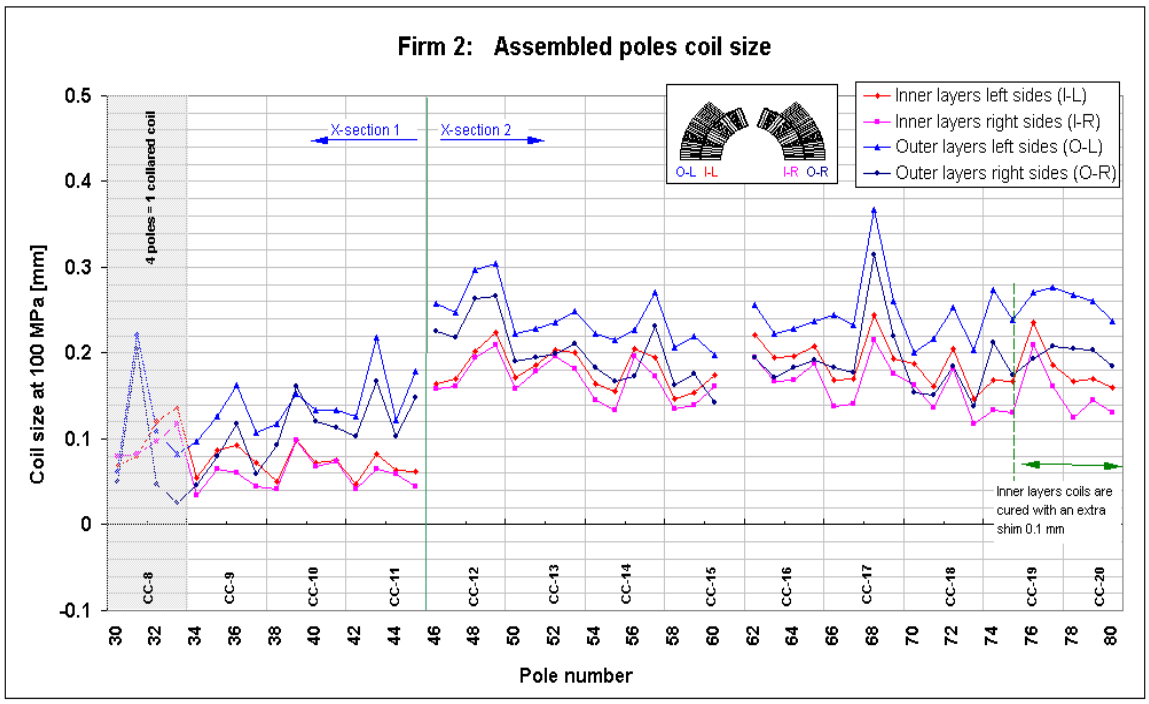


Fig.3 Firm 2. Average coil size in the straight part of the assembled poles (50 poles).

Firm 3. Up to now, only 8 assembled poles are measured with the IMMG press, but due to the problem of instability of the displacement transducers values in this machine, the measurement data could not be used for analysis. IMMG is working on this problem.

### 1.2.2 Measurements on single layers

Firm 1. At this firm, due to the design of coil size-measuring machine, only the assembled poles are measured, and no single layers.

Firm 2. The jump, which has already been observed before on the assembled poles, now also turned up on the inner layer coils just after switching to the X-section 2 coil design (fig. 4). However, here is no evidence, that this jump is due to the change of the coil cross-section, as there is also a jump on the outer layer coil dimensions (fig. 5). This is happen at about the same period of production. As can be seen in the fig. 3-5, the coil size, especially on the inner layers, is too big, and as a corrective action, starting from the inner layer 75, the coils were cured with extra shim 0.1 of mm in the curing mould, later, similar action was taken also for the outer layers coils, starting from the outer layer 98 (fig. 5).

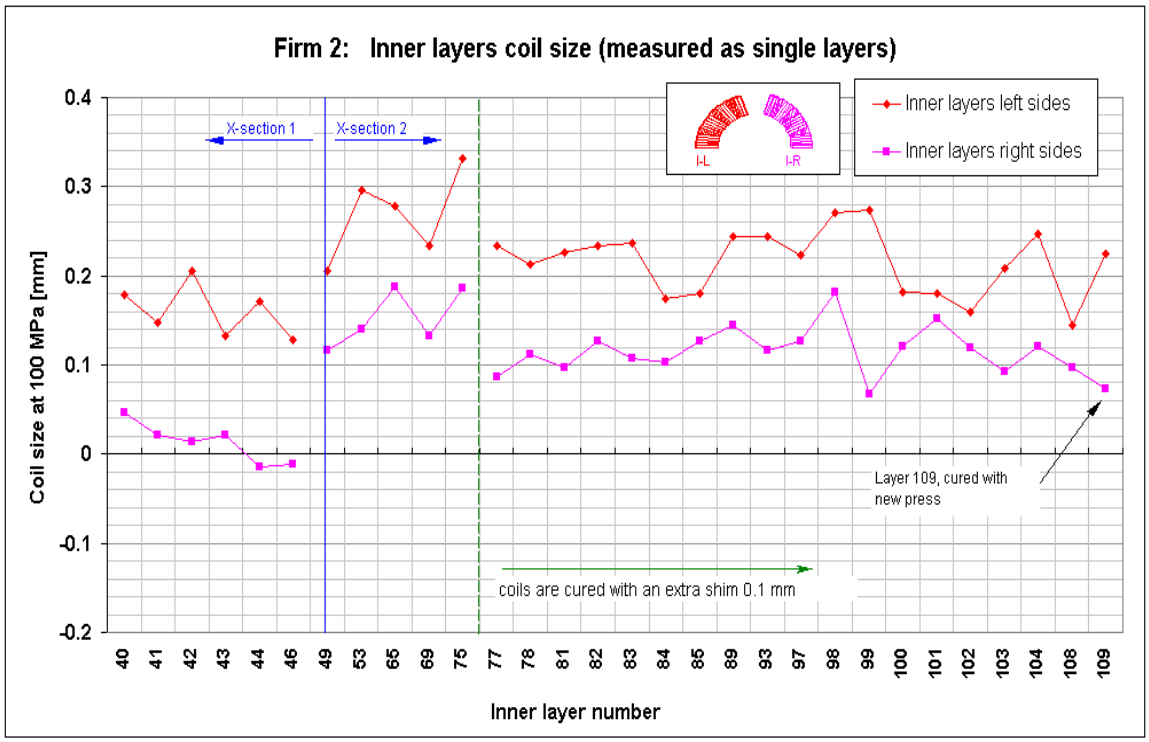


Fig.4 Firm 2. Average coil size in the straight part of the inner layers

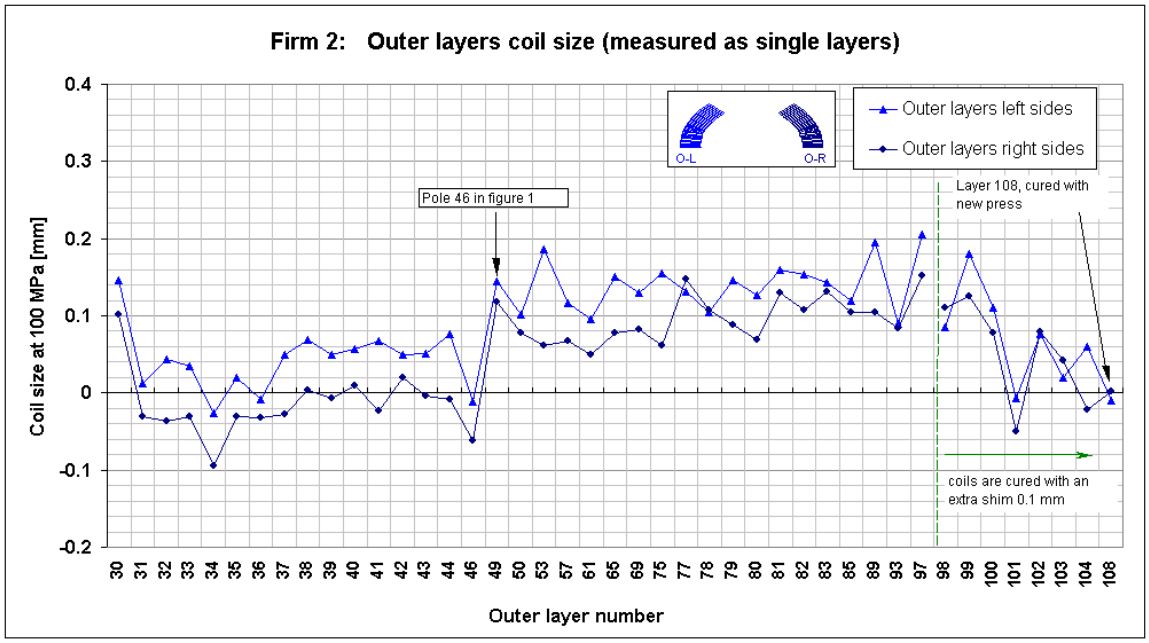


Fig.5 Firm 2. Average coil size in the straight part of the outer layers.

Firm 3. So far, among the three contractors, firm 3 is producing the coils with the smallest variation in the average coil size, especially on the outer layers: from 60 layers, which are measured, the coils size stays within a range of 0 - 0.15 mm. However, a jump is observed in the inner layer coil size after switching to the X-section 2 coil design (fig. 6). This particular case was investigated in greater depth. In fact, the trend of the E-modulus of the coil is following the one of the coil size, only with an opposite sign (note that in fig. 7, the scale of E-modulus is inversed). Moreover, when the coils size suddenly increased between the layers 154 and 155, the E-modulus of these coils drops, which means that those coils become less rigid. If the origin of the increase in coil size is due to change of the copper wedges design, i.e. due to an increase of their thickness, the composite E-modulus of the coil should also rise (as there will be more copper in percentage). However, the opposite is observed: the E-modulus does not increase, but reduces. Consequently, it is more likely that the increase of the coil size is caused by the change of the insulation thickness. In orders to prove that, all the batches number of the cables, the insulation tapes and the copper wedges were checked out and it was found that the jump in the coil size between inner layers 154 and 155 is due to the change of the cable insulation adhesive tape from *Kapton* to *Pixeo* with a nominal thickness of 68.52 microns, and an allowed tolerance range of +/- 3 %). The difference in the thickness of the two types of tape is up to 2 microns (see graph in Annex 1), which is only half of the allowed tolerances range, but adds up on 15 turns of the inner layer to 60 microns of extra thickness on the coil size.

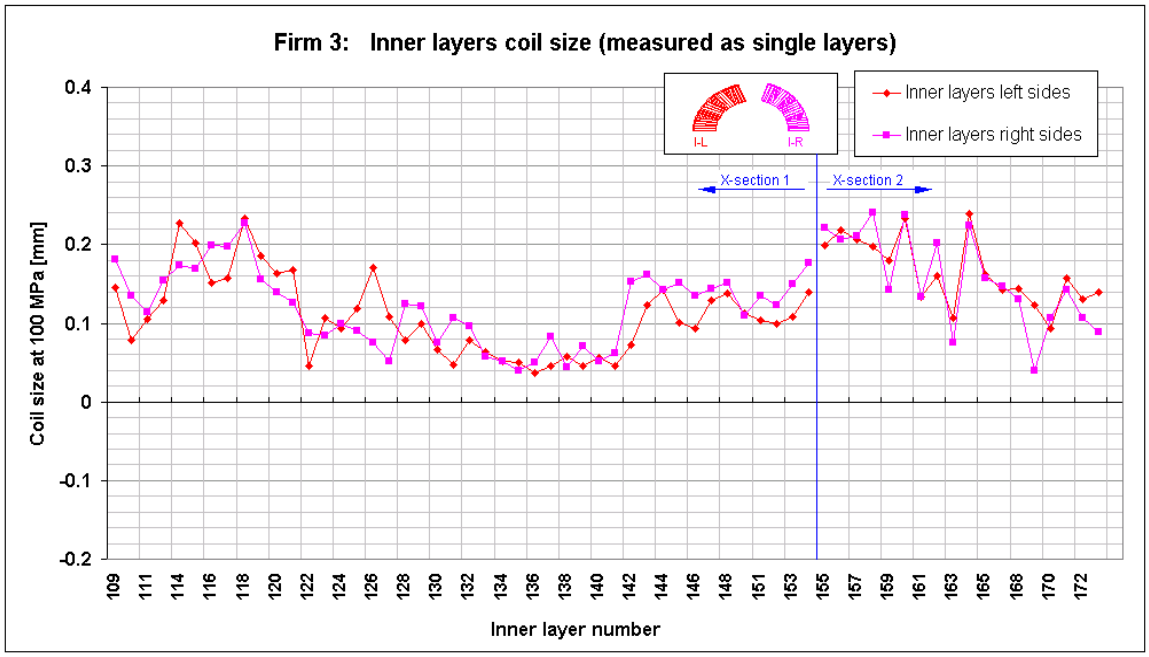


Fig.6 Firm 3. Average coil size in the straight part of the inner layers.

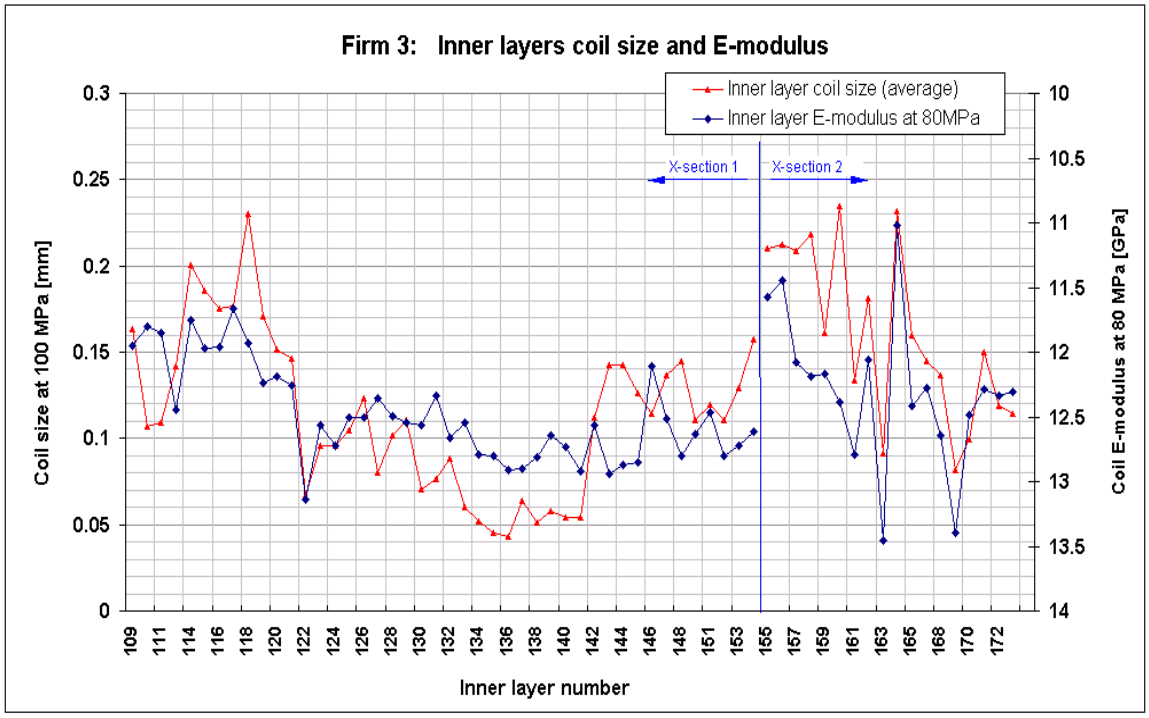


Fig.7 Firm 3. Average coil size and coil E-modulus in the straight part of the inner layers.

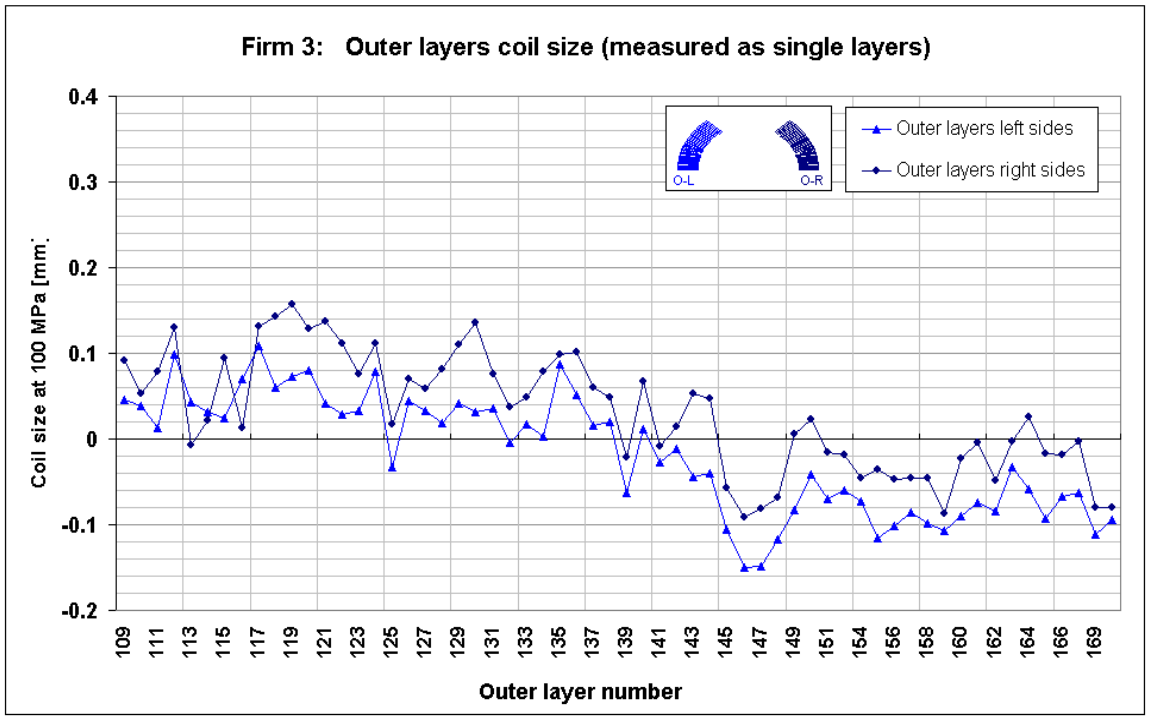


Fig.8 Firm 3. Average coil size in the straight part of the outer layers.

## 1.3 Size tolerances of the coil cross-section along the coil

The size of the coil cross-section of single layers or assembled poles is typically measured in 14-20 longitudinal positions along the coil. The "systematic" longitudinal coil profile, which is calculated as an average longitudinal coil profile for the batches of 30-50 coils, shows that despite the rather big variation of the coil size during mass production (trends), the longitudinal shape of coils made with the same tooling is rather stable. This "systematic" longitudinal coil profile is unique for each manufacturer and comes from the tooling tolerances (winding mandrels and curing moulds). In the figs. 9 and 10 we could see, that the inner and outer layers № 109 and № 108 have similar shapes to the previous coils, even if they were cured in the new curing press.

The "signature" of the tooling is different on the left and right hand sides of the coils as well as on both layers (see figs. 9-16).

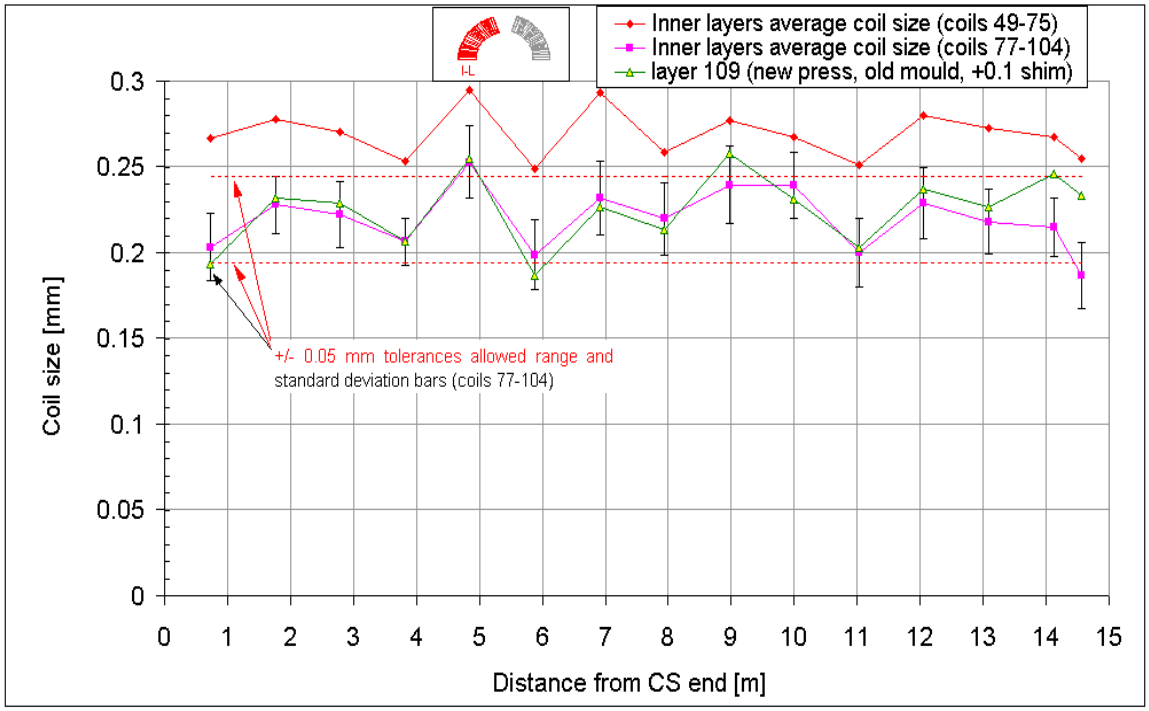


Fig.9 Firm 2. "Systematic" longitudinal coil profile for the inner layers left side (Curing mould 1).

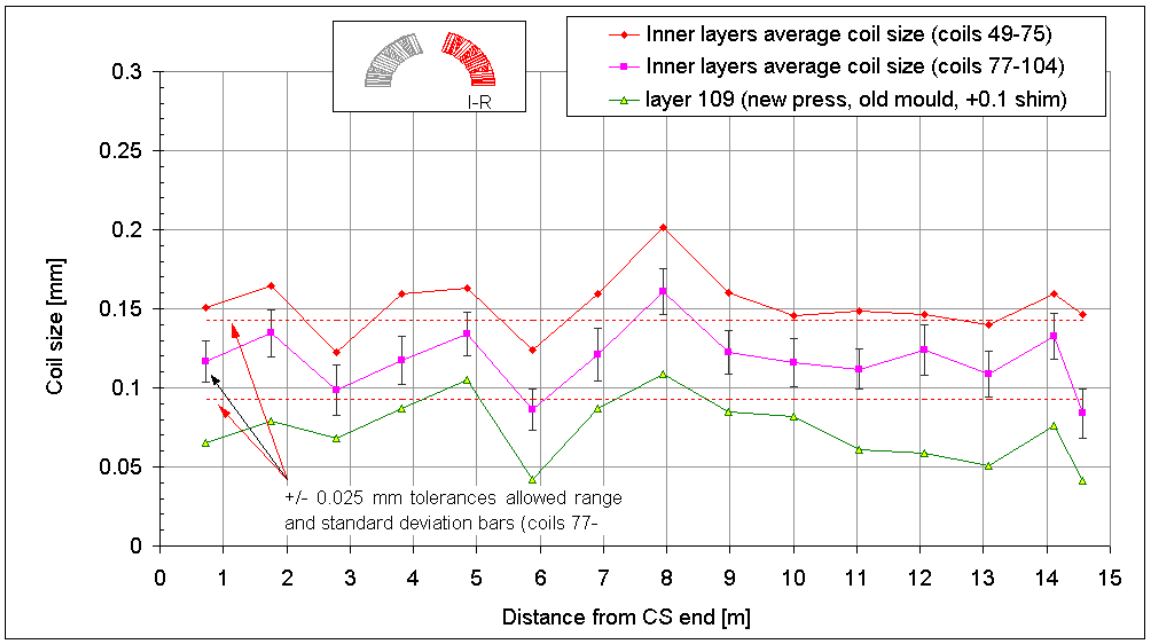


Fig. 10 Firm 2. "Systematic" longitudinal coil profile for the inner layers right side (Curing mould 1).

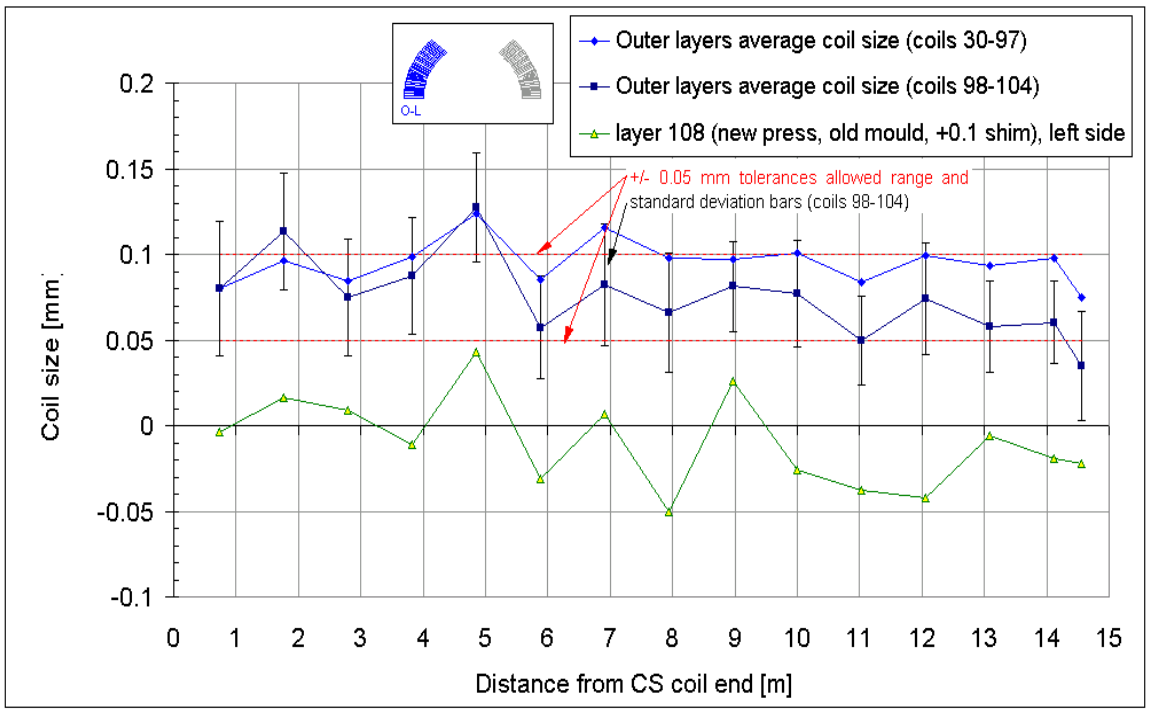


Fig. 11 Firm 2. "Systematic" longitudinal coil profile for the outer layers left side (Curing mould 1).

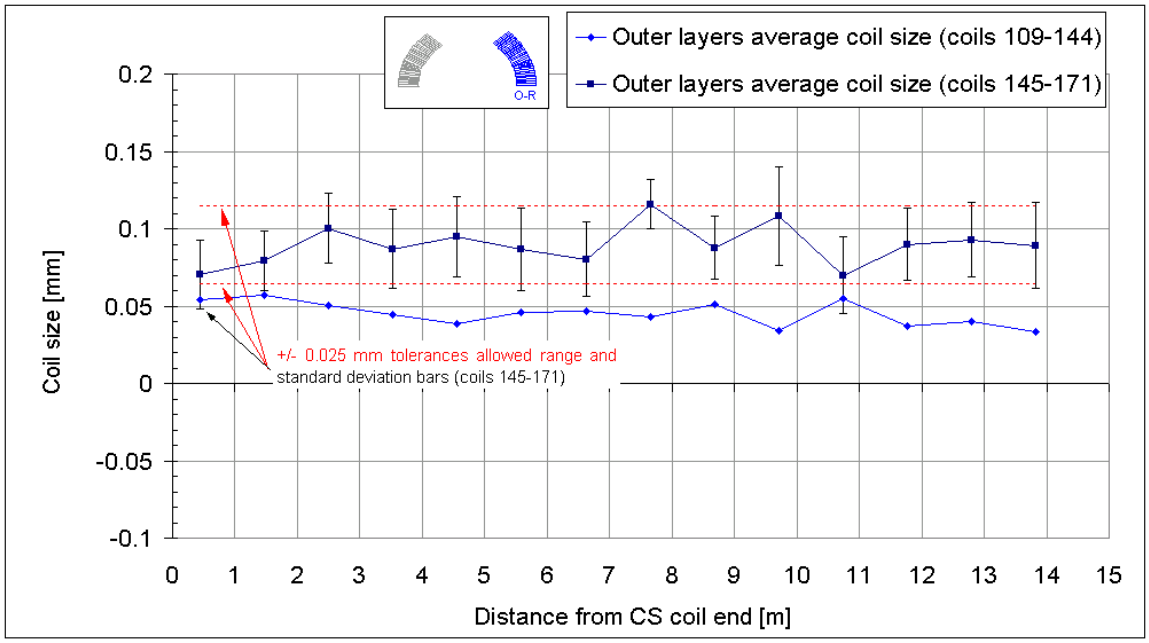


Fig. 12 Firm 2. "Systematic" longitudinal coil profile for the outer layers right side (Curing mould 1).

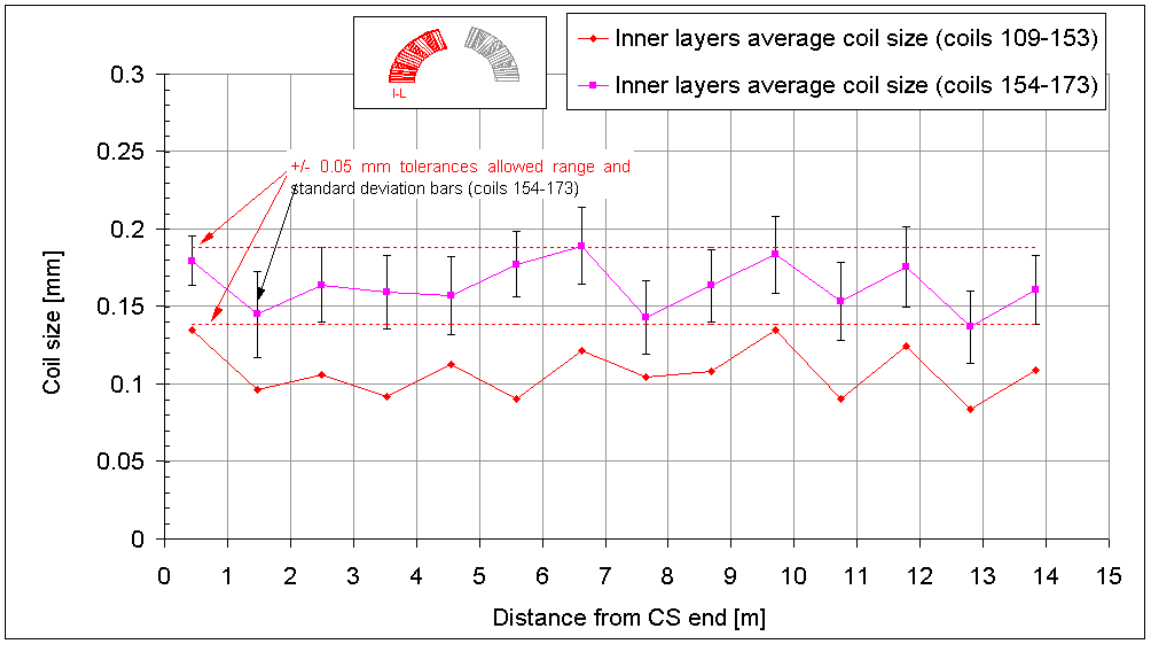


Fig. 13 Firm 3. "Systematic" longitudinal coil profile for the inner layers left side (Curing mould 1).

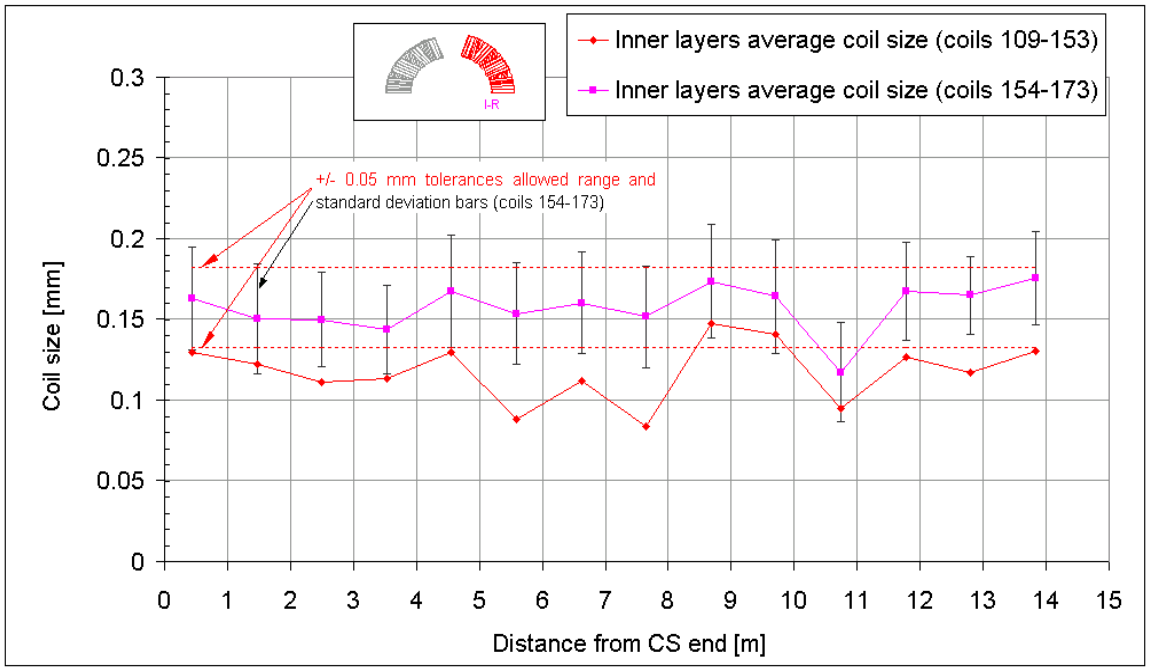


Fig. 14 Firm 3. "Systematic" longitudinal coil profile for the inner layers right side (Curing mould 1).

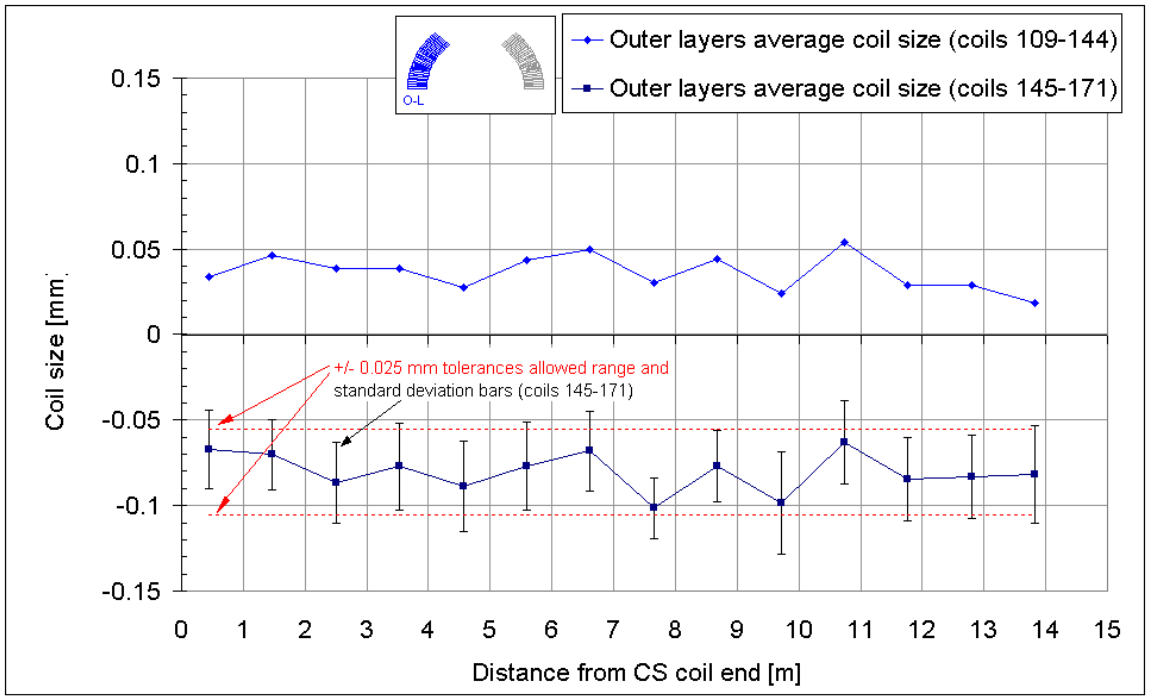


Fig. 15 Firm 3. "Systematic" longitudinal coil profile for the outer layers left side (Curing mould 1).

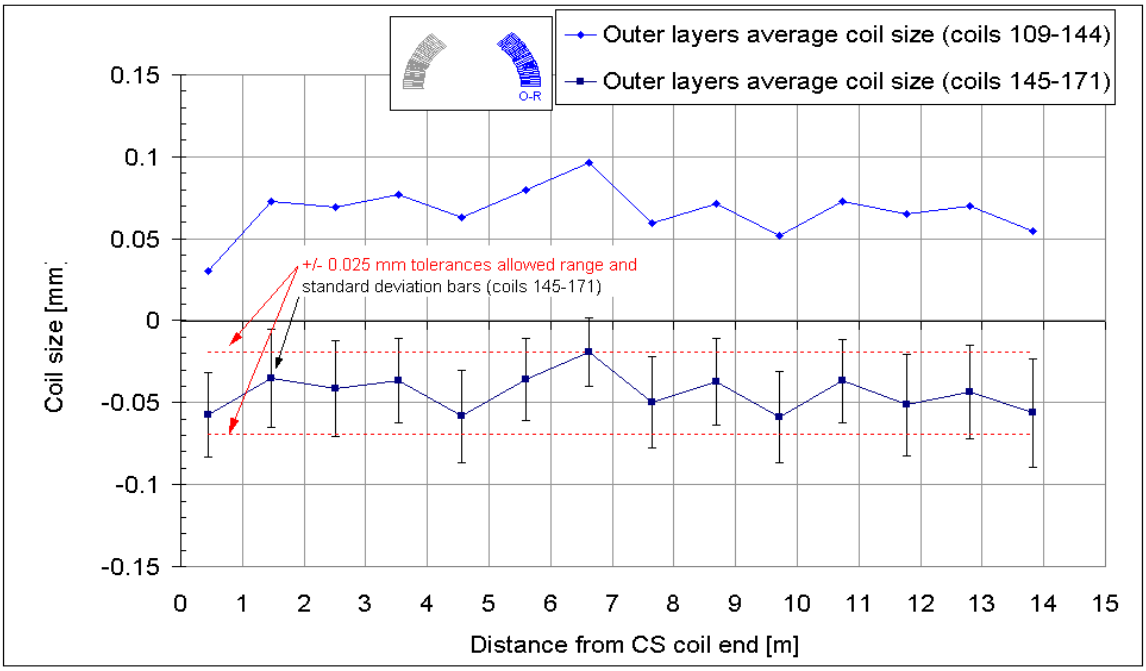


Fig. 16 Firm 3. "Systematic" longitudinal coil profile for the outer layers right side (Curing mould 1).

## 1.4 Left-to-right side coil asymmetry in the collared coils

Firm 1. In average, the left-to-right side coil asymmetry which is measured on the poles is in the order of 0.04-0.06 mm. However, for some poles the difference in the size between left and right sides of inner layer coils goes up to 0.2 mm! (see for example, the poles № 41 and № 94 in fig. 2). The inner layer coils systematically have the left side bigger then the right side whereas on the outer layer coils it is the other way. Therefore, being assembled into the magnets, the upper and lower poles coil size tolerances are averaged, nevertheless the total left–to-right sides asymmetry stays in the order of 0.04-0.06 mm (fig. 17-18). This results in tilt of the magnet midplane. In principle, this tilt should affect the *a3* field multipole, however, no such correlation can be found from warm magnetic measurements. This could be due to a low measuring accuracy or due to other components tolerances of the collared coil which are not taken into consideration here. Nevertheless, up to now, the *a3* multipole is not in a critical path as it is well inside its allowed range (see report of E.Todesco).

Firm 2. The inner layer coils, which are measured as single layers show a rather big left-to-right side asymmetry: up to 0.1 mm (see fig. 3). When both layers are assembled into the pole, this asymmetry being partially smoothed by the outer layer becomes less than 30-40 microns (fig.5).

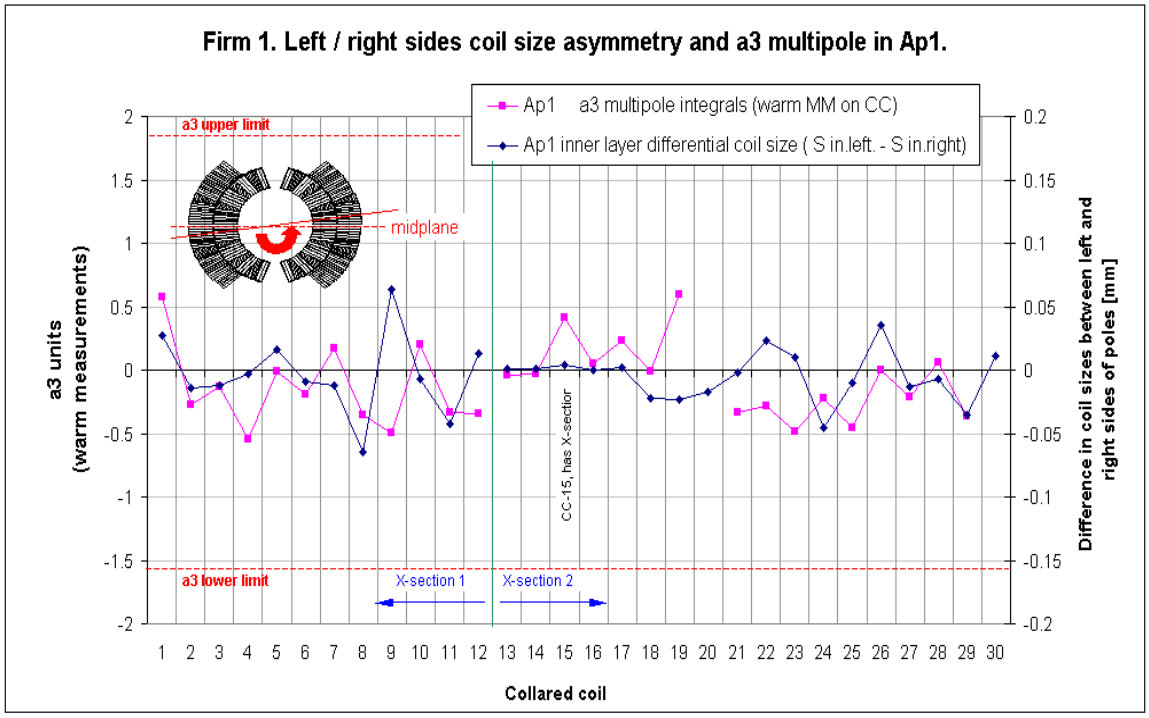


Fig. 17 Firm 1. Expected left-to-right side coil size asymmetry in the collared coil (Aperture 1) and measured a3 multipole (warm magnetic measurements).

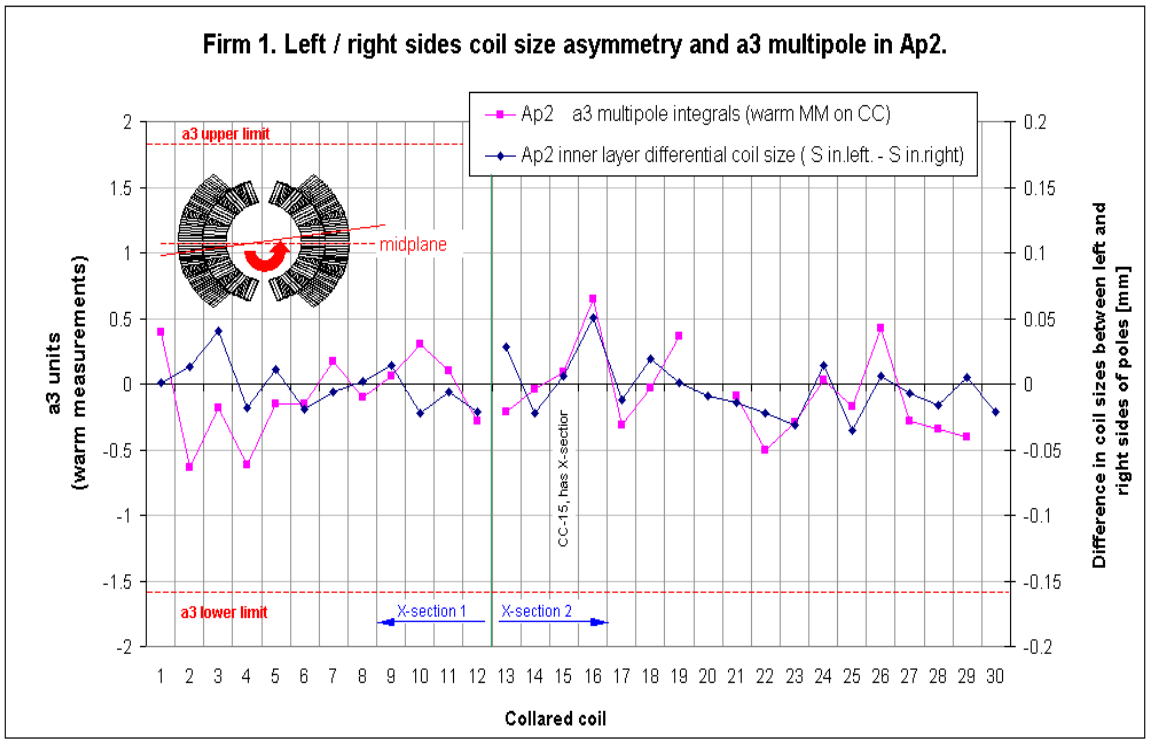


Fig. 18 Firm 1. Expected left-to-right side coil size asymmetry in the collared coil (Aperture 2) and measured a3 multipole (warm magnetic measurements).

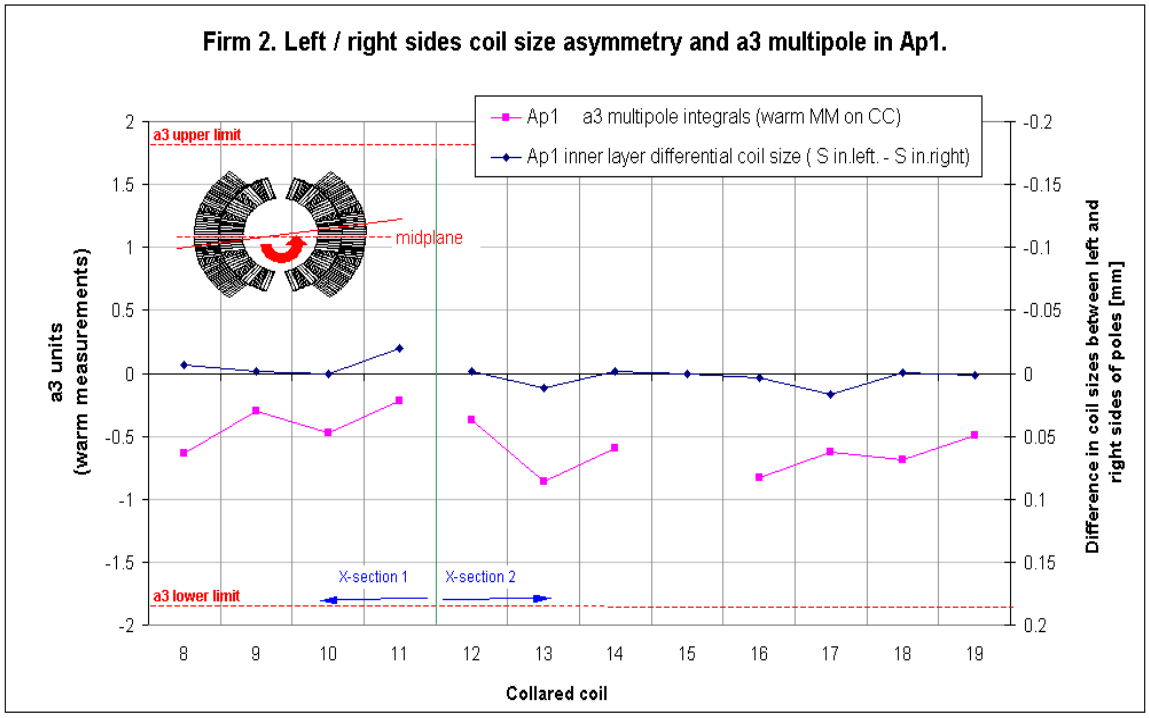


Fig. 19 Firm 1. Expected left-to-right side coil size asymmetry in the collared coil (Aperture 1) and measured a3 multipole (warm magnetic measurements).

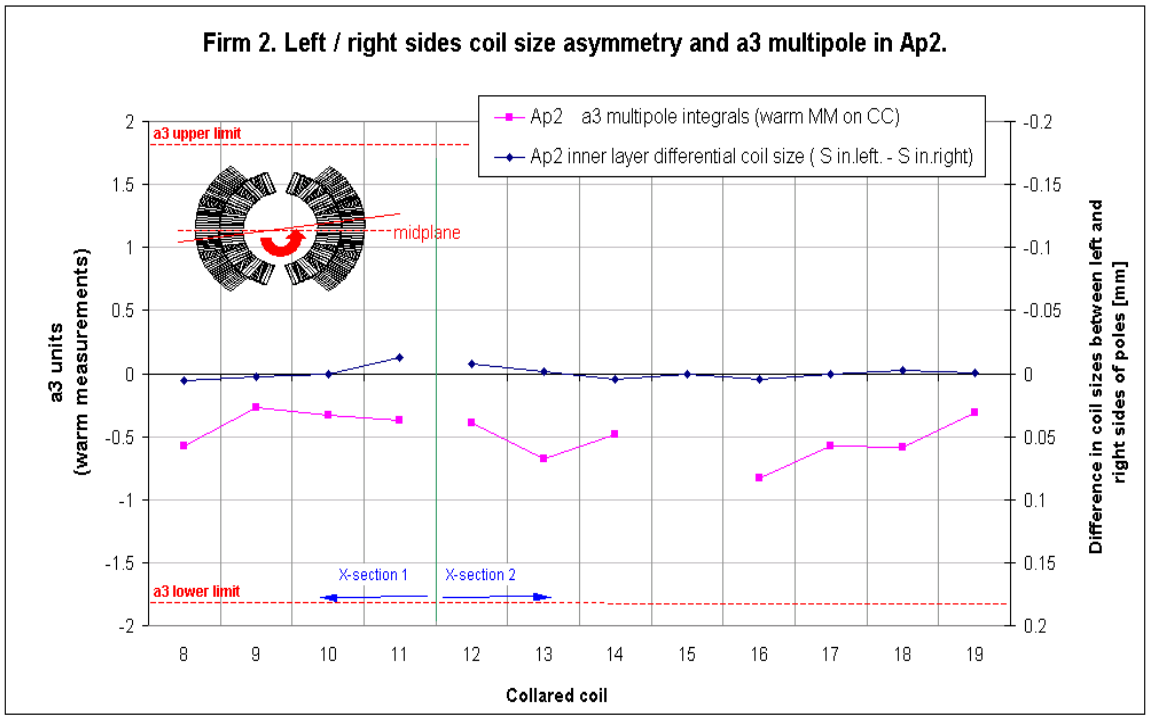


Fig. 20 Firm 1. Expected left-to-right side coil size asymmetry in the collared coil (Aperture 1) and measured a3 multipole (warm magnetic measurements).

## 1.5 Up/down coil asymmetry in the collared coils

The difference on the average coil sizes between two poles assembled into one aperture of the magnet produces an up/down asymmetry and results in a shift of the magnet midplane. In magnetic measurements this shift is seen as a non-zero value of the skew quadrupole (*a2*). Due to the fact, that the allowed range for *a2* multipole is smaller then for *a3*, the up/down coil asymmetry in the magnets is more crucial compared to the one of the left/right sides.

Firm 1. Considering the data on coils sizes, a rather big up/down asymmetry of up to 0.15 mm is expected. This asymmetry arises from two sources: the big random coil size variation shown which is in fig. 2 and from the fact that the poles which are going into the magnet assembly are not sorted for an optimum coil geometry. In fact, typically, for a new magnet assembly, the companies do not have a big stock of poles; often only 4 poles are available. In the magnet assembly, these 4 poles are arranged into the collared coil structure by simply following the pole number ascending order (first aperture upper pole *n*, lower one n+1 end so on), without any sorting. This procedure results in a big spread in *a2* multipole values, exceeding in some magnets its allowed range (for example CC-15 and 17 in fig.22). As an exercise, a rearrangement of the 4 poles in the CC-15 has been carried out, aiming to have the best possible up/down symmetry in both apertures of this magnet. As a result, we could get a magnet with two times smaller up/down asymmetry (see figs. 22 and 23). Such a way of field quality optimization in a magnet is almost cost free and thus should be recommended for use in the companies.

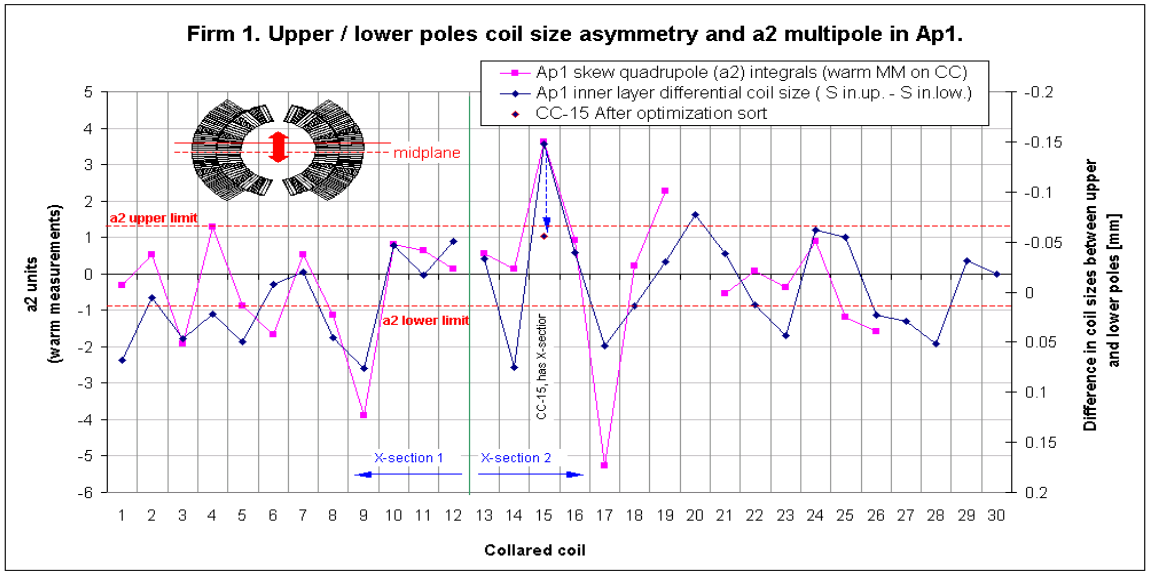


Fig. 21 Firm 1. Expected up/down coil size asymmetry in the collared coil (Aperture 1) and measured a2 multipole (warm magnetic measurements).

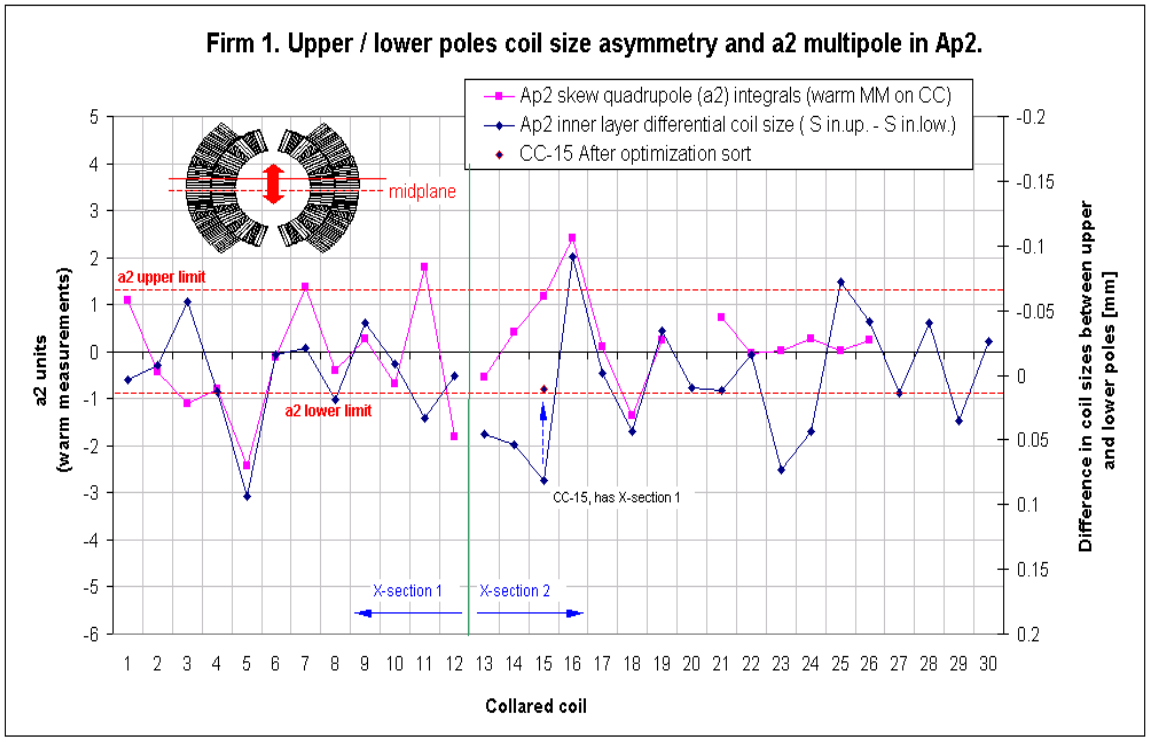


Fig. 22 Firm 1. Expected up/down coil size asymmetry in the collared coil (Aperture 2) and measured a2 multipole (warm magnetic measurements).

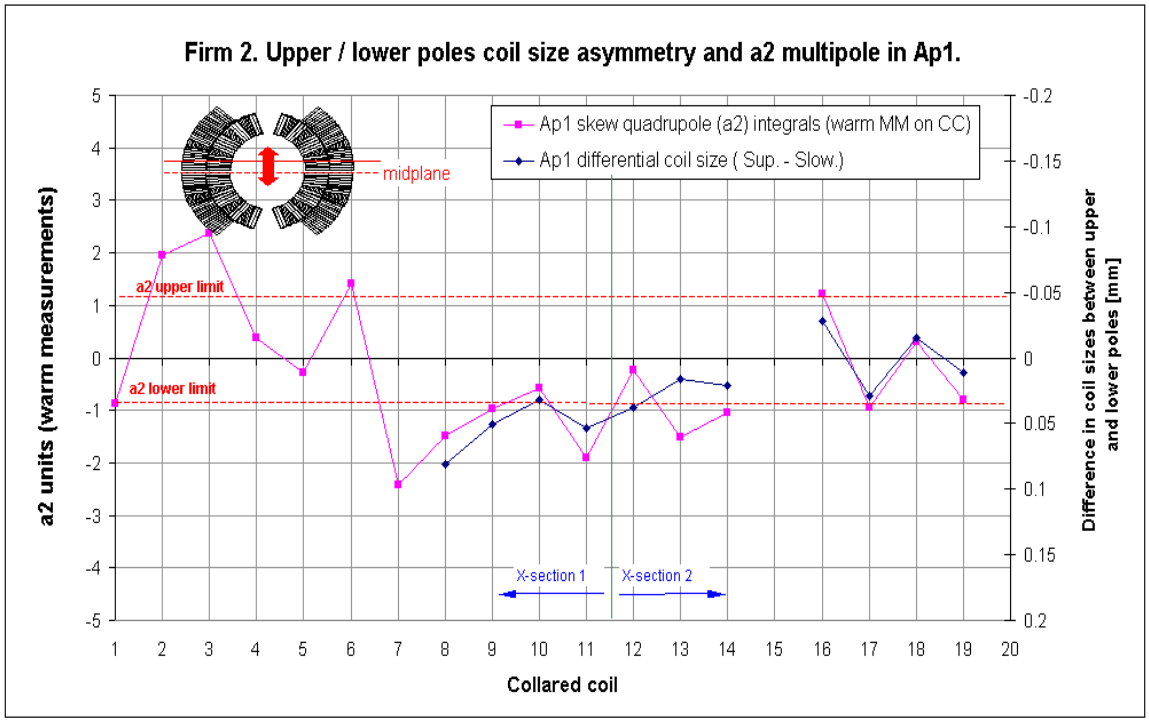


Fig. 23 Firm 2. Expected up/down coil size asymmetry in the collared coil (Aperture 1) and measured a2 multipole (warm magnetic measurements).

Firm 2**.** At this firm the coil size on poles is measured with the IMMG presses starting from the CC-8. As can be seen in the fig. 24 and 25, the up/down coil asymmetry is a bit smaller, compared to firm 1.

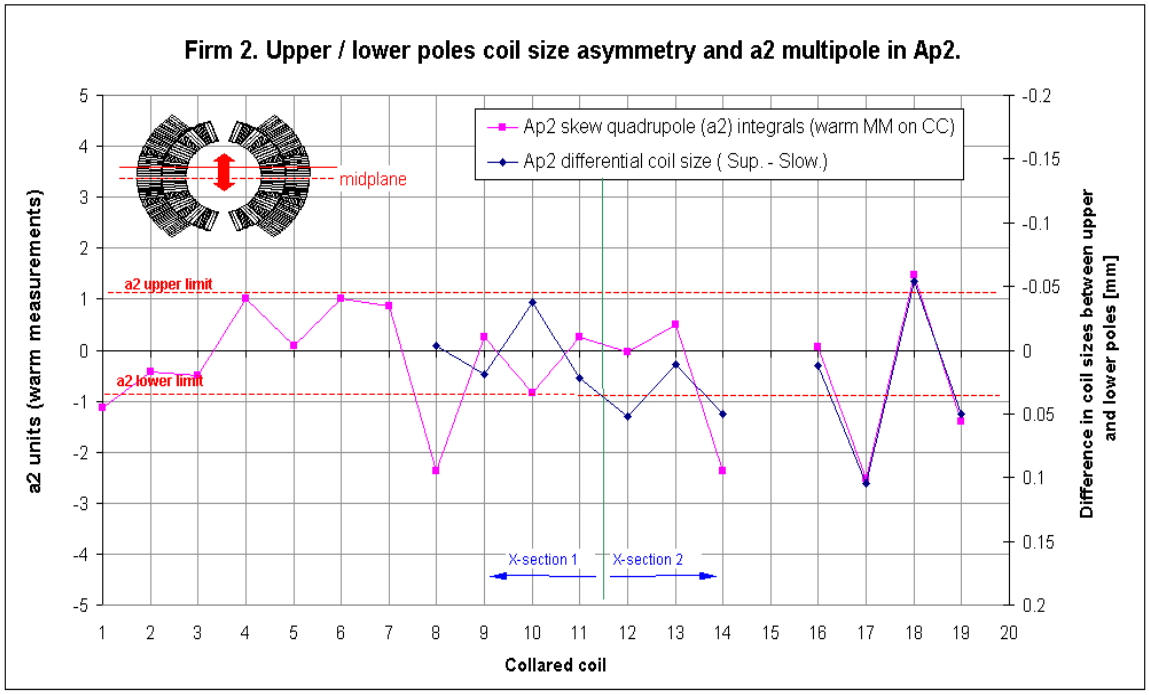


Fig. 24 Firm 2. Expected up/down coil size asymmetry in the collared coil (Aperture 2) and measured a2 multipole (warm magnetic measurements).

Firm 3. No measurements on the poles available yet.

## 2. Measurement data of the collared coil dimensions

### 2.1 Trend graphs (straight part of the coil)

The measured dimensions of the collared coils after collaring are functions of the coil pre-stress. Due to coil pre-stress the collars expand. The collared coils dimensions (later CC dimensions) are measured at 10 (see Fig. 25) points in 50-80 positions in the longitudinal direction. In all figures, the CC dimensions are given not in absolute values, but relative to their nominal value. In fact, the collars itself have production tolerances, which are not taken into account here (the analysis of the influence of collars dimensions and other components tolerances on the magnet field quality is under way in MMS/MA section and will be given in a separate paper).

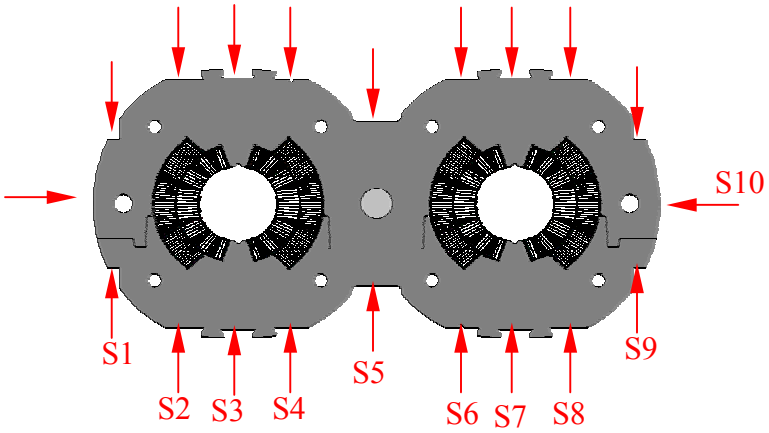


Fig. 25 Measurement points of the collared coil dimensions

Firm 1. The CC dimensions are measured in 40 pre-defined positions along the coil, where 25 positions are taken in the straight part of the coil (each 0.5 m). Up to now, all the measurements are taken manually. The average on CC dimensions for measuring points S2-S4 (aperture 1) and S6-S8 (aperture 2) are shown in fig. 26 together with the average coil size. There is a rather good correlation between CC dimensions and coil size apart of the first three magnets. In these magnets non-nominal polar shims (bigger ones) were used during the magnet assembly.

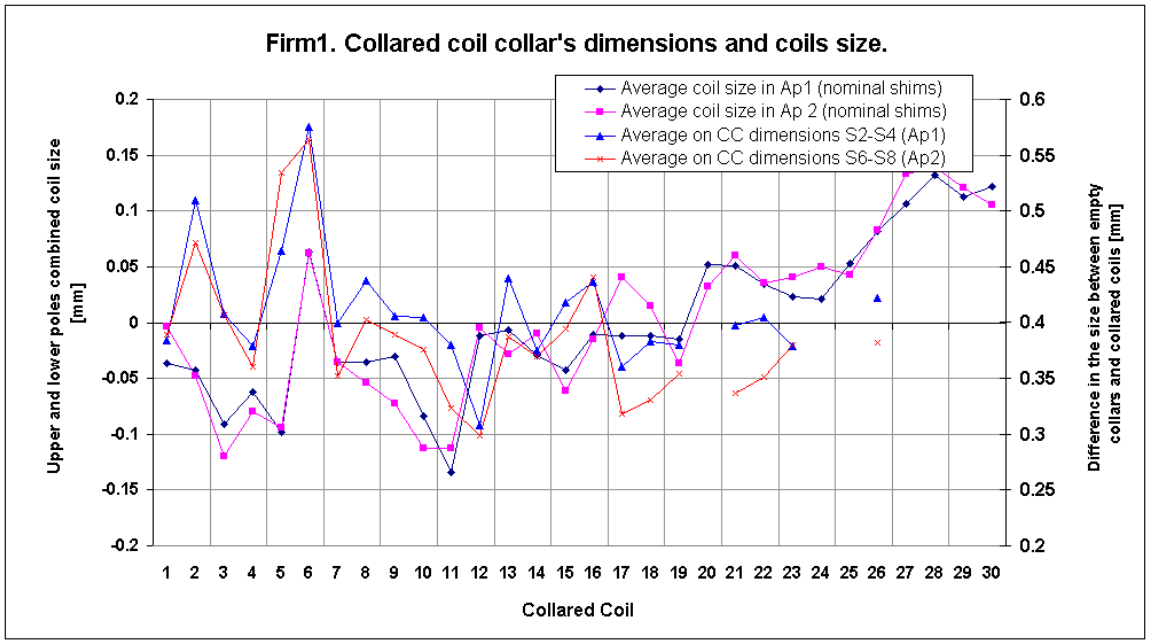


Fig. 26 Firm 1. Collared coil dimensions (difference in vertical size between empty collars and collared coil) and average coil size.

Firm 2. The CC dimensions are measured in 78 pre-defined positions along the coil, where 54 positions are taken in the straight part of the coil (each 0.25 m). For the first 7 collared coils the measurements were done manually, whereas starting from the CC-8, the automated measuring machine is in use. The average on CC dimensions for measuring points S2-S4 (aperture 1) and S6-S8 (aperture 2) are shown in fig. 27 together with the average coil size. The data on the coils size is taken from the measurements done on assembled poles, which are available only from the magnet 8 on. The thickness of the polar shims is taken into account.

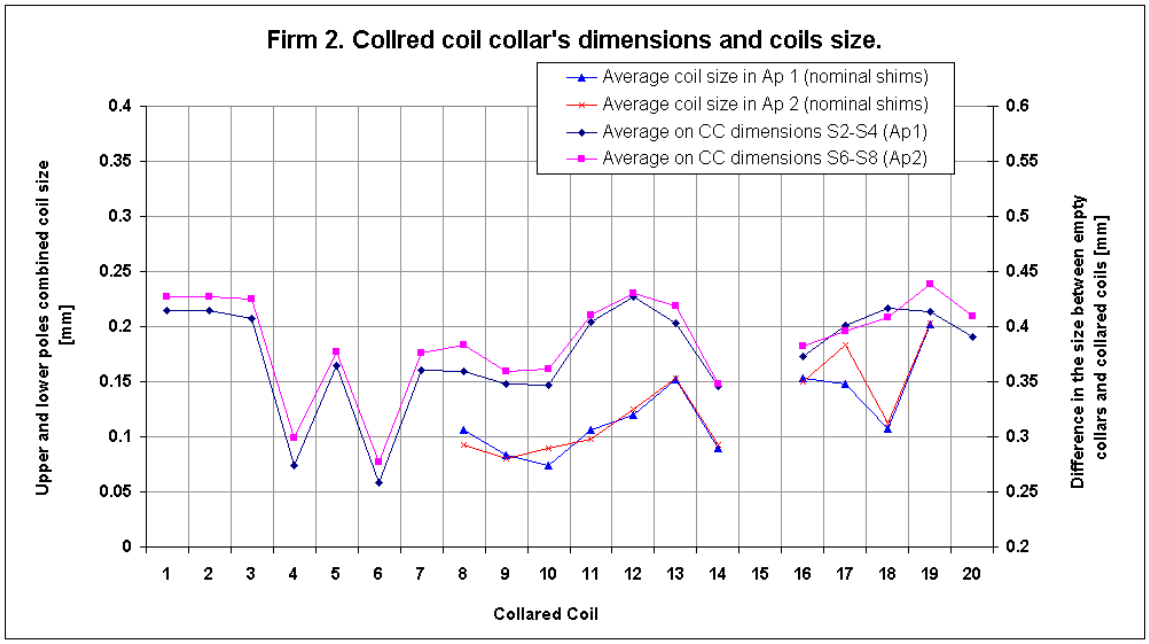


Fig. 27 Firm 2. Collared coil dimensions (difference in vertical size between empty collars and collared coil) and average coil size (only available for CC-8 –19).

Firm 3. The CC dimensions are measured in 44 pre-defined positions along the coil, where 28 positions are taken in the straight part of the coil (each 0.5 m). All collared coils are measured with the automated measuring machine. For post-processing and transfer of data to CERN the firm is using the Collared Coil Database software package, which was developed by CERN. The average on CC dimensions for measuring points S2-S4 (aperture 1) and S6-S8 (aperture 2) are shown in fig. 28 together with the average coil size. The data on the coils size is taken from the measurements, which are done on individual layers, as there is no data available yet on assembled poles. The thickness of the polar shims is taken into account.

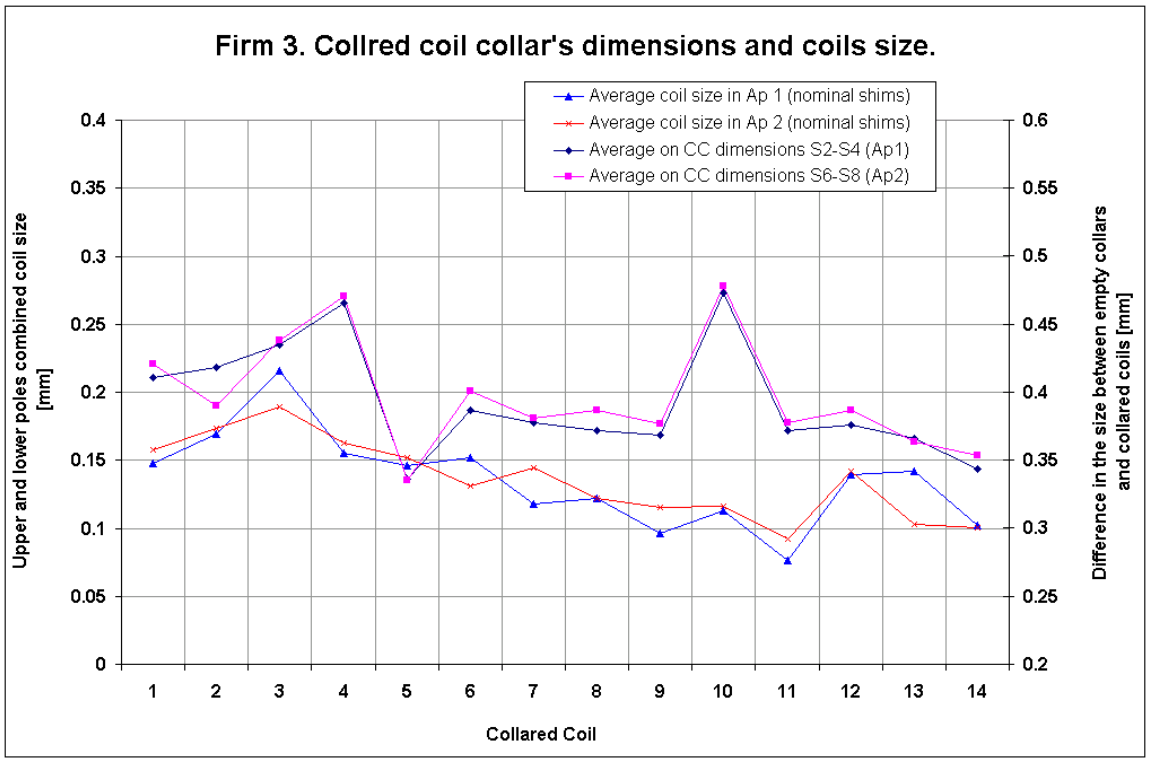


Fig. 28 Firm 3. Collared coil dimensions (difference in vertical size between empty collars and collared coil) and average coil size (measured on single layers).

## 2.2 Collared Coil dimensions tolerances along the coil

During collaring, the peak pressure in the coil is reaching values of 140-160 MPa. At such pressures, the insulations of the cable creeps and the coil shape, which is given by the curing mould (see chapter 1.3), is modified by the collaring pressure profile along the coil. Typically, due to some particularities of the collaring process, the coils at the extremities are compressed more (and thus the insulation creeps more) than in the mid of the magnet. Consequently, the coil goes into a kind of banana shape. Despite the high rigidity of the stainless steel collars, and due to the variation of the pre-stress in the coil, this shape of the coil can be well observed in the profile of the collared coil dimensions. There is a good correlation between the mechanical and the magnetic measurement data on this fact. In fig. 29 (firm 2) we could see that the systematic on the normal decapole *b5* is well matching the shape of the collared coil. The change of the coil X-section just gives a shift on *b5*, but the coil shape stays the same (fig. 30).

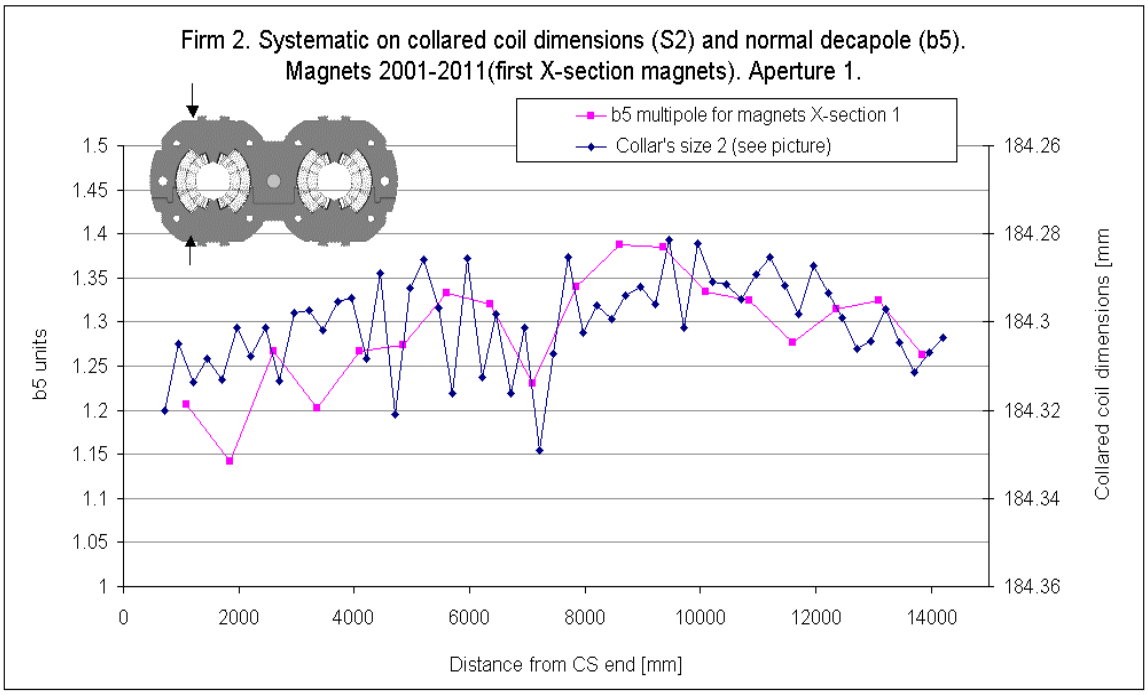


Fig. 29 Firm 2. Statistical collared coil longitudinal profile and systematic on normal decapole in aperture 1. (coil x-section 1, magnets only)

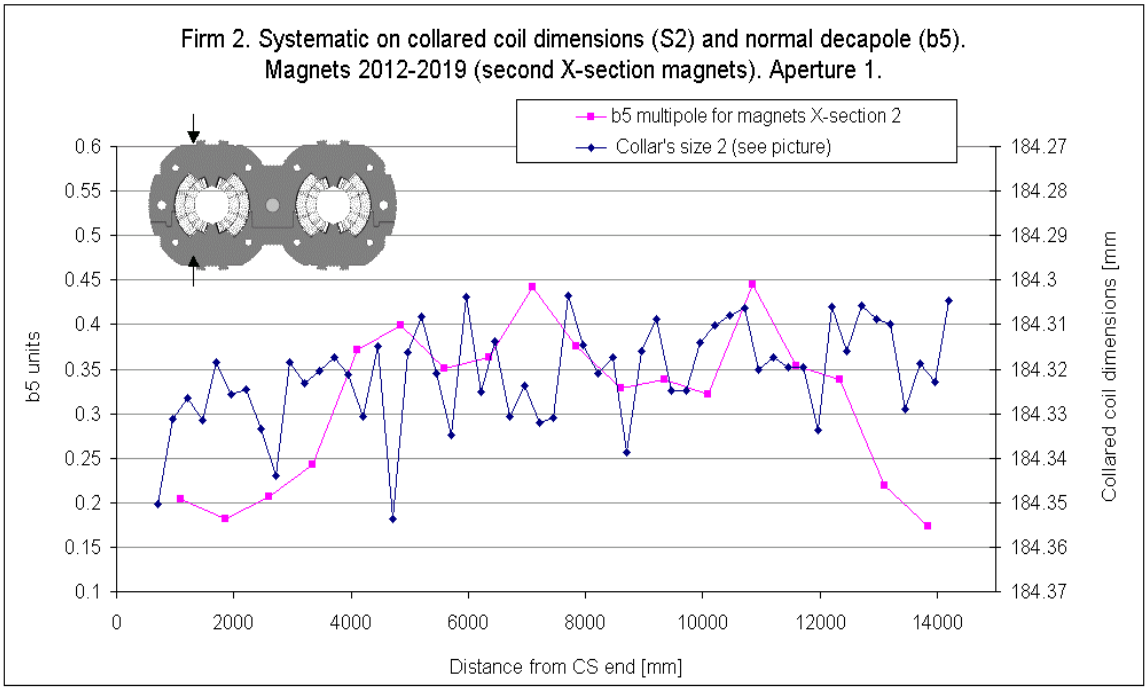


Fig. 30 Firm 2. Statistical collared coil longitudinal profile and systematic on normal decapole in aperture 1. (coil x-section 2, magnets only)

## 3. Acknowledgments

We wish to acknowledge P. Fessia, A. Musso, L. Rossi, W. Scandale, D. Tommasini, C. Vollinger and R. Wolf for comments, discussions and valuable help.

# Annex 1